Molecular Therapy
Oncolytics
Original Article

Neoadjuvant Use of Oncolytic Herpes Virus G47Δ Enhances the Antitumor Efficacy of Radiofrequency Ablation

Tomoharu Yamada,[1,2] Ryosuke Tateishi,[2] Miwako Iwai,[1] Kazuhiko Koike,[2] and Tomoki Todo[1]

[1]Division of Innovative Cancer Therapy, Advanced Clinical Research Center, The Institute of Medical Science, The University of Tokyo, Tokyo 108-8639, Japan; [2]Department of Gastroenterology, Graduate School of Medicine, The University of Tokyo, Tokyo 113-8655, Japan

G47Δ is a triple-mutated oncolytic herpes simplex virus type 1 designed to induce antitumor immune responses efficiently. We examine the usefulness of G47Δ as a neoadjuvant therapy for radiofrequency ablation (RFA), a standard local treatment for certain cancers such as liver cancer, but remote recurrences within the same organ often occur. In A/J mice harboring bilateral subcutaneous Neuro2a tumors, the left tumors were treated with G47Δ intratumoral injections followed by RFA. Whereas the RFA-treated tumors were all eradicated, the growth of the right tumors was evaluated and tumor-infiltrating lymphocytes were analyzed. The G47Δ+RFA treatment caused smaller volumes of right tumors, accompanied by increased $CD8^+/CD45^+$ T cells, compared with G47Δ monotherapy. After depletion of $CD8^+$ T cells, the enhanced efficacy on the contralateral tumors was completely abolished. Neoadjuvant G47Δ led to rejection of rechallenged tumors, which was caused by efficient induction of specific antitumor immune responses shown by enzyme-linked immunospot (ELISPOT) assays. Treatment of tumor-harboring animals with an anti-programmed cell death 1 ligand 1 (PD-L1) antibody led to even greater efficacy on contralateral tumors. Our study indicates that the neoadjuvant use of G47Δ effectively enhances the efficacy of RFA via $CD8^+$ T cell-dependent immunity that is further augmented by an immune checkpoint inhibitor.

INTRODUCTION

Oncolytic viruses can selectively replicate in and kill cancer cells. Oncolytic herpes simplex virus type 1 (HSV-1) is attractive for cancer therapy, because it infects a wide variety of cell types, exhibits strong cytotoxicity, and induces antitumor immune responses. Genetically engineered HSV-1 with multiple mutations exhibits minimal toxicity to normal tissues, which is important for clinical application. G47Δ is a triple-mutated, third-generation oncolytic HSV-1 constructed from G207, a double-mutated HSV-1, by adding another deletion mutation within the nonessential *α47* gene. The third mutation conferred improved replication capability in cancer cells and augmentation of antitumor immunity, resulting in an enhanced antitumor effect of G47Δ while maintaining the safety profile.[1] G47Δ has been shown to have efficacy in a variety of solid cancers *in vivo* and to kill cancer stem cells.[2–4] G47Δ has been tested in clinical trials in Japan, including those for glioblastoma, prostate cancer, olfactory neuroblastoma, and malignant mesothelioma,[5] and a phase II trial has recently shown a high efficacy in residual or recurrent glioblastoma patients. Among other oncolytic viruses, talimogene laherparepvec (T-VEC), a double-mutated oncolytic HSV-1 expressing granulocyte-macrophage colony-stimulating factor (GM-CSF), showed a significantly higher durable response rate in patients with advanced melanoma when injected repeatedly into the tumors compared with control patients who received subcutaneous injections of GM-CSF, and was approved by the US Food and Drug Administration (FDA) as a new drug in 2015.[6] An oncolytic poliovirus reportedly generated long-term survival in a portion of patients with glioblastoma in a phase I trial,[7] and an oncolytic vaccinia virus seemed effective in patients with hepatocellular carcinoma (HCC) in a phase II trial but failed to show the efficacy in a phase III trial that followed.[8] Oncolytic HSV-1 has shown efficacy for HCC in preclinical studies.[9,10] Thus, oncolytic viruses, including G47Δ, seem promising for a variety of cancers, although they are yet to be developed for HCC.

Radiofrequency ablation (RFA) is widely used for cancer treatment.[11] Especially for HCC, RFA is considered the standard local treatment.[12] Although a recurrence of HCC at an RFA-treated site is rare, remote new lesions often appear within the liver.[13] Many agents such as c-MET inhibitors, immune checkpoint inhibitors (ICIs), and Toll-like receptor 9 agonists reportedly enhance the antitumor effect of RFA, but none of them is considered efficacious enough to be a standard combination partner for RFA, and new agents that can reduce remote recurrence after RFA treatment are yet to be developed.[14–16] The FDA approved nivolumab, an ICI, for HCC in 2017. In a phase I/II trial, the disease control rate was greater than 50%, but the objective response rate was less than 20%.[17] Whereas RFA is reported to release tumor-associated antigens,[18,19] clearly, an additional treatment that can turn those non-responsive "cold" tumors "hot" is required.

Received 18 March 2020; accepted 19 August 2020;
https://doi.org/10.1016/j.omto.2020.08.010.

Correspondence: Tomoki Todo, MD, PhD, Division of Innovative Cancer Therapy, Advanced Clinical Research Center, The Institute of Medical Science, The University of Tokyo, 4-6-1 Shirokanedai, Minato-ku, Tokyo 108-8639, Japan.
E-mail: toudou-nsu@umin.ac.jp

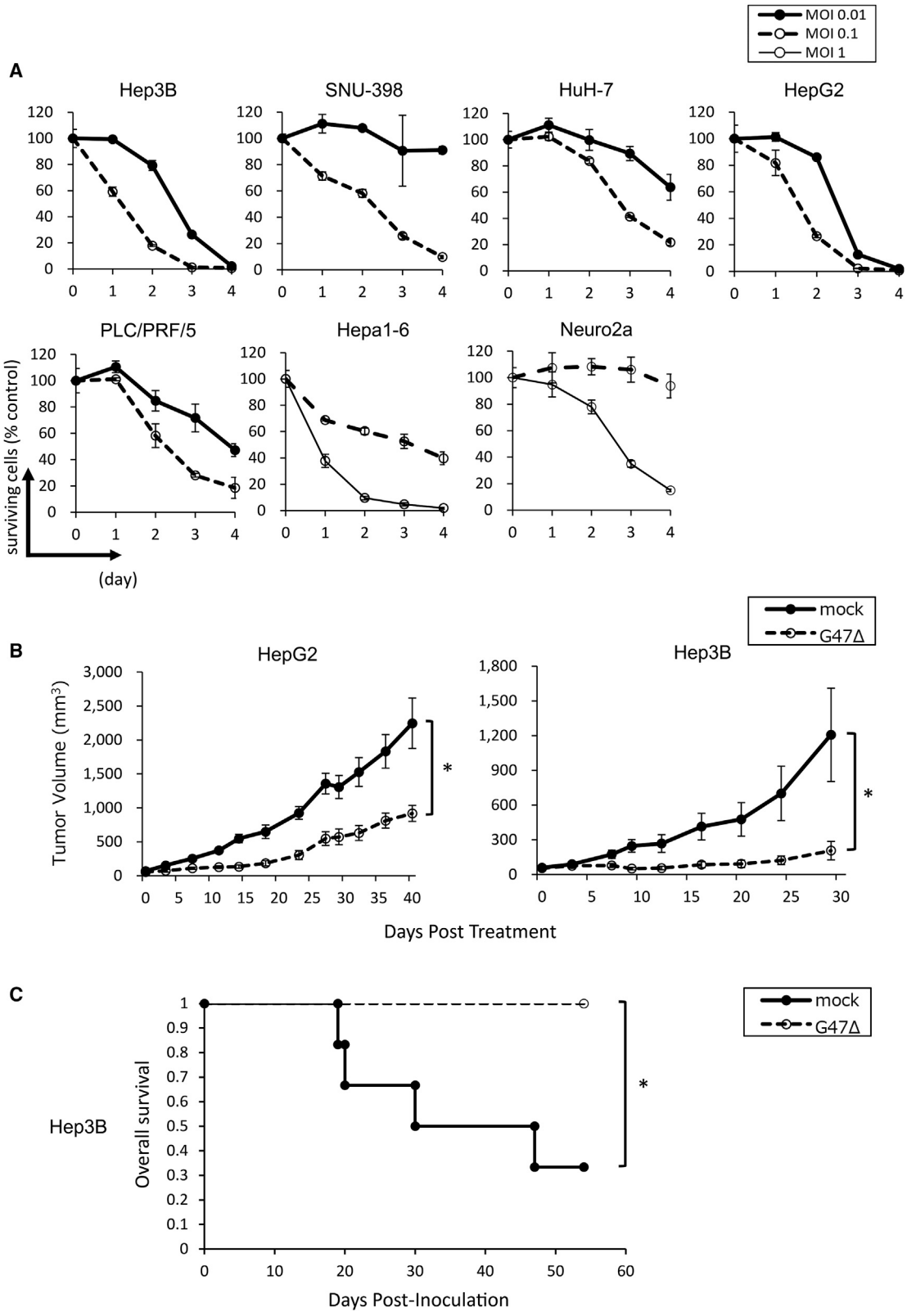

(legend on next page)

Oncolytic HSV-1 can elicit specific antitumor immunity in the course of cancer cell-selective viral replication, and therefore a combination with various ICIs is being investigated.[20] In a mouse brain tumor model, the efficacy of G47Δ-expressing murine interleukin (IL)-12 was enhanced by a combination with ICI.[21] In a phase Ib clinical trial, the efficacy of T-VEC in advanced melanoma patients was improved by a combination with an anti-programmed cell death 1 (PD-1) antibody. In the successful cases, those tumors that received T-VEC injections showed infiltration of interferon (IFN)-γ-producing $CD8^+$ T cells.[20] Another report showed that the antitumor immunity elicited by oncolytic Maraba virus was maintained after the resection of virus-injected tumors in a mouse subcutaneous tumor model, suggesting that oncolytic virus therapy prior to surgery can reduce tumor recurrence.[22] In this study, we examined the usefulness of G47Δ as a neoadjuvant therapy for RFA and, furthermore, ICIs as a booster.

RESULTS

G47Δ Exerts Broad Oncolytic Activity against Human HCC Cell Lines

Because RFA is the current standard local treatment for HCC, we first sought to perform this study in models using HCC cells. To evaluate the cytopathic effect of G47Δ on HCC *in vitro*, five human HCC cell lines (Hep3B, SNU-398, HuH-7, HepG2, and PLC/PRF/5), a murine HCC cell line (Hepa1-6), and a murine neuroblastoma cell line (Neuro2a) were used. The cells were infected with G47Δ at a multiplicity of infection (MOI) of 0.1 or 0.01. G47Δ showed cytopathic activity in all cell lines tested, killing more than 80% of cells by day 4 after infection at a MOI of 0.1 in all cell lines tested, and more than 35% at a MOI of 0.01, except for SNU-398 cells (Figure 1A). To evaluate the infectivity with G47Δ, X-gal (5-bromo-4-chloro-3-indolyl β-D-galactoside) staining was performed in the six HCC cell lines, plus Vero cells as control, after infection with G47Δ at a MOI of 1 or 3. G47Δ efficiently infected all cell lines evaluated (Figure S1A). We further examined the replication capabilities of G47Δ, and all HCC cell lines tested except for SNU-398 ($p = 0.061$) showed significantly better virus yields at 48 h compared with 24 h (Figure S1B).

G47Δ Is Efficacious for Human HCC *In Vivo*

Established subcutaneous tumors of HepG2 or Hep3B in athymic mice were injected intratumorally with G47Δ (2×10^6 plaque-forming units [PFU]) on days 0 and 3. In both the HepG2 and Hep3B subcutaneous tumor models, G47Δ exhibited significant antitumor effects, indicating that these HCCs are highly susceptible to G47Δ treatment *in vivo* (Figure 1B).

To mimic the clinical settings, orthotopic tumors were generated in athymic mice using Hep3B cells and were treated with a single intratumoral injection with G47Δ (2×10^6 PFU) on day 35. For each animal, the abdominal cavity was opened at the time of injection, the established tumor in the liver was confirmed, and G47Δ was injected under direct view into the tumor. G47Δ treatment significantly improved the overall survival of the tumor-bearing mice compared with mock treatment (Figure 1C). Necropsy at the time of death confirmed that all animals died from tumor burden. These results suggest that G47Δ is useful for the treatment of human HCC.

Neoadjuvant Use of G47Δ in Combination with RFA Improves the Antitumor Efficacy in Immunocompetent Mice

Next, we hypothesized that the antitumor immunity induced by intratumoral injection with G47Δ prior to RFA would enhance the antitumor efficacy of RFA. Because an immunocompetent tumor model is necessary to test the hypothesis, we initially tried to use a murine HCC cell line, MH134-TC. Bilateral subcutaneous tumors were generated in C3H mice and the left tumors were treated with RFA or sham-RFA on day 4. However, regardless of whether the RFA treatment was performed, all contralateral right tumors shrank after day 15, indicating that MH134-TC cells were too immunogenic and the model was inappropriate for this study (Figure S2). Two other murine HCC cell lines, Hepa1-6 and BNL, did not form subcutaneous tumors consistently in respective syngeneic mice (data not shown). Because none of the murine HCC cell lines available, including MH134-TC that formed subcutaneous tumors, was suitable for generating a tumor model for RFA, we decided to use poorly immunogenic, HSV-1-susceptible Neuro2a cells for this proof-of-concept study. Using A/J mice with established bilateral subcutaneous tumors of syngeneic Neuro2a, the left tumors were treated with intratumoral injections with G47Δ (2×10^6 PFU) or mock on days 6, 8 and 10, followed by RFA on day 12. In all RFA-treated animals, with or without neoadjuvant G47Δ, the treated tumors are eradicated, and no local recurrence is observed by day 26, so the contralateral tumor growth is followed in this study (Figure 2A). In all sham-RFA-treated animals, the sham-treated tumors grew, and the tumor growth could be inhibited with G47Δ monotherapy (data not shown). G47Δ monotherapy inhibited the growth of the contralateral, non-treated tumors significantly compared with control or RFA monotherapy on day 18 (G47Δ versus control, $p < 0.01$; G47Δ versus RFA, $p < 0.05$). Mice with tumors that reached 20 mm in diameter in mock-treated groups were sacrificed on day 18, whereas G47Δ-treated groups could be followed until day 24. RFA monotherapy did not demonstrate a significant antitumor effect on the contralateral tumors by day 18 (RFA versus control, $p = 0.12$ on day 18). The G47Δ + RFA

Figure 1. The Antitumor Effect of G47Δ on Human Hepatocellular Carcinoma

(A) Cytopathic effect of G47Δ *in vitro*. Monolayers of human cell lines (Hep3B, SNU-398, HuH-7, HepG2, and PLC/PRF/5) and murine cell lines (Hepa1-6 and Neuro2a) in six-well plates were infected with G47Δ at a MOI of 0.01, 0.1, or 1. Surviving cells were counted using a Coulter counter on the indicated days, and expressed as the percentage of the number of mock-infected control cells. The results are the means; bars indicate SD. (B) Antitumor activity of G47Δ (2×10^6 PFU) in BALB/c *nu/nu* mice bearing subcutaneous HepG2 or Hep3B tumors. Tumors established in the left flanks (HepG2 average, 63 mm^3; Hep3B average, 58 mm^3) were treated with intratumoral injections with G47Δ on days 0 and 3. Tumor growth was evaluated by measuring the tumor size twice a week. The results are the means (n = 7); bars represent SEM. Tumor volume = length × width × height × $^1/_2$. *$p < 0.05$. (C) In BALB/c *nu/nu* mice with orthotopic Hep3B tumors, a single intratumoral injection with G47Δ led to a longer survival than did a mock injection (n = 6 and 7, respectively).

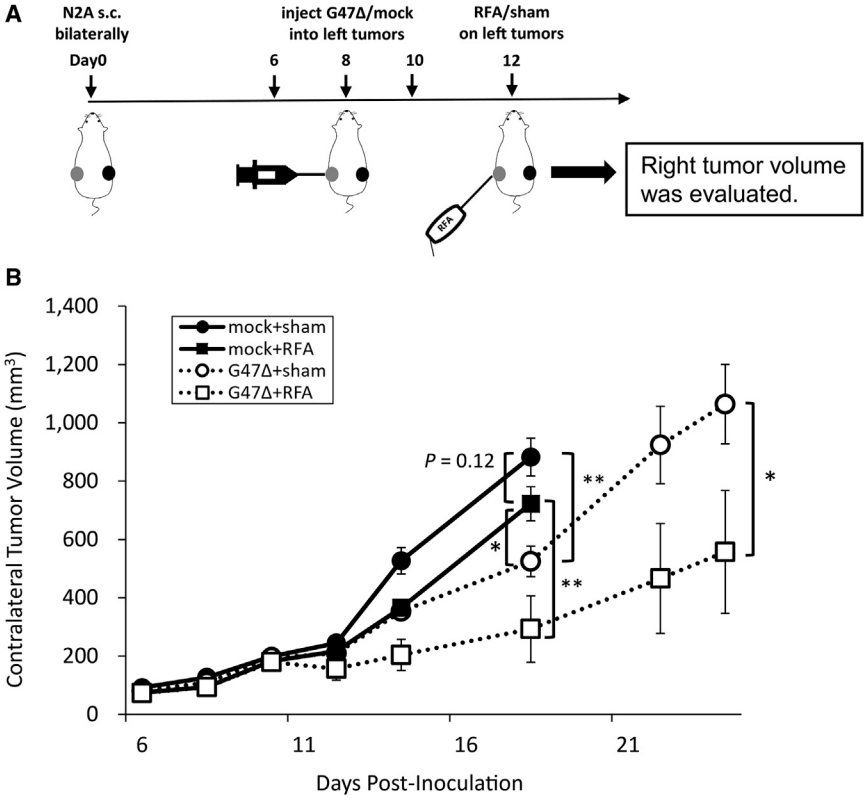

Figure 2. Antitumor Effect of Neoadjuvant G47Δ in Combination with RFA in A/J Mice Bearing Bilateral Subcutaneous Neuro2a Tumors

(A) When bilateral subcutaneous Neuro2a tumors reached 6–8 mm in diameter (left tumor average, 79 mm^3), the left tumors were treated with intratumoral injections with G47Δ (2×10^6 PFU) or mock on days 6, 8, and 10 followed by RFA or sham treatment on day 12. RFA completely eradicated the treated tumors, so the tumor growth on the right, non-treated side was followed. (B) The G47Δ + RFA combination therapy inhibited the growth of contralateral tumors significantly compared with each monotherapy on day 24. The data are means (n = 6); bars indicate SEM. *p < 0.05, **p < 0.01.

combination therapy caused a greater reduction in the contralateral tumor volume compared with each monotherapy (G47Δ + RFA versus RFA, p < 0.01 on day 18; G47Δ + RFA versus G47Δ, p < 0.05 on day 24) (Figure 2B). The expected and observed fractional tumor volumes (FTVs) on day 18 were 0.486 and 0.332, respectively. As the expected FTV to observed FTV ratio was greater than 1 (1.47), G47Δ and RFA therapies were considered to have a synergistic effect.

Neoadjuvant G47Δ in Combination with RFA Results in Recruitment of $CD8^+$ T Cells and an Increase in Serum IFN-γ Levels

To explore the immunological impact of neoadjuvant G47Δ in combination with RFA on the contralateral tumors, we evaluated tumor-infiltrating lymphocytes (TILs) in these tumors by flow cytometric analysis and determined the numbers of $CD8^+$ T cells, $CD4^+$ T cells, natural killer cells, regulatory T cells, and helper T cells among $CD45^+$ lymphocytes (Figure S3). The proportion of $CD8^+$ T cells among $CD45^+$ cells was significantly increased by G47Δ monotherapy compared with control or RFA monotherapy (G47Δ versus control, p < 0.01; G47Δ versus RFA, p < 0.05). The combination therapy further increased the proportion of $CD8^+$ T cells among $CD45^+$ cells compared with each monotherapy (G47Δ + RFA versus RFA, p < 0.01; G47Δ + RFA versus G47Δ, p < 0.05; Figure 3A). The proportion of regulatory T cells of the combination therapy was smaller than that of the control (p < 0.01), although it was not significantly different from either monotherapies (Figure 3B). Moreover, histological analysis of the $CD8^+$ T cell in the contralateral tumors revealed greater infiltration of $CD8^+$ T cells after G47Δ + RFA combination therapy compared with the monotherapies (Figure 3C). The number of $CD8^+$ cells was significantly increased in the combination therapy (G47Δ + RFA versus G47Δ, p < 0.05; G47Δ + RFA versus RFA, p < 0.001; Figure 3D).

Next, we examined the serum cytokine levels to evaluate the systemic immune responses. Serum collected from mice bearing subcutaneous tumors at 1, 3, and 7 days after RFA from all treatment groups was analyzed for IL-6 and the pro-inflammatory T helper (Th)1-related cytokines, IFN-γ and IL-12. IFN-γ was significantly elevated by the combination therapy compared with each monotherapy on postoperative day (POD) 7 (G47Δ + RFA versus G47Δ, p < 0.01; G47Δ + RFA versus RFA, p < 0.01; Figure 3E). For IL-12, the combination therapy did not cause any significant difference between other therapies. However, the combination therapy significantly decreased the IL-6 level compared with RFA monotherapy on POD 3 (p < 0.01; Figure S4).

$CD8^+$ T Cell Depletion Abolishes the Augmented Antitumor Effect by the Combination Therapy

To examine the contribution of $CD8^+$ T cells to the augmented antitumor effect by the combination therapy, A/J mice harboring bilateral subcutaneous Neuro2a tumors were depleted of $CD8^+$ T cells by intraperitoneal injections with an anti-CD8 monoclonal antibody initiated 1 day before G47Δ injection (Figure 4A). The augmented antitumor effect of G47Δ + RFA in the right, non-treated tumors was completely abolished after depletion of $CD8^+$ T cells (G47Δ + RFA + anti-CD8 versus G47Δ + RFA + immunoglobulin G [IgG]2a control, p < 0.01), suggesting that $CD8^+$ T cells are required for the augmented antitumor effect of the combination therapy (Figure 4B).

Neoadjuvant G47Δ in Combination with RFA Leads to Rejection of Tumor Rechallenge

Next, we examined whether neoadjuvant use of G47Δ in combination with RFA can prevent tumor recurrence. To mimic remote

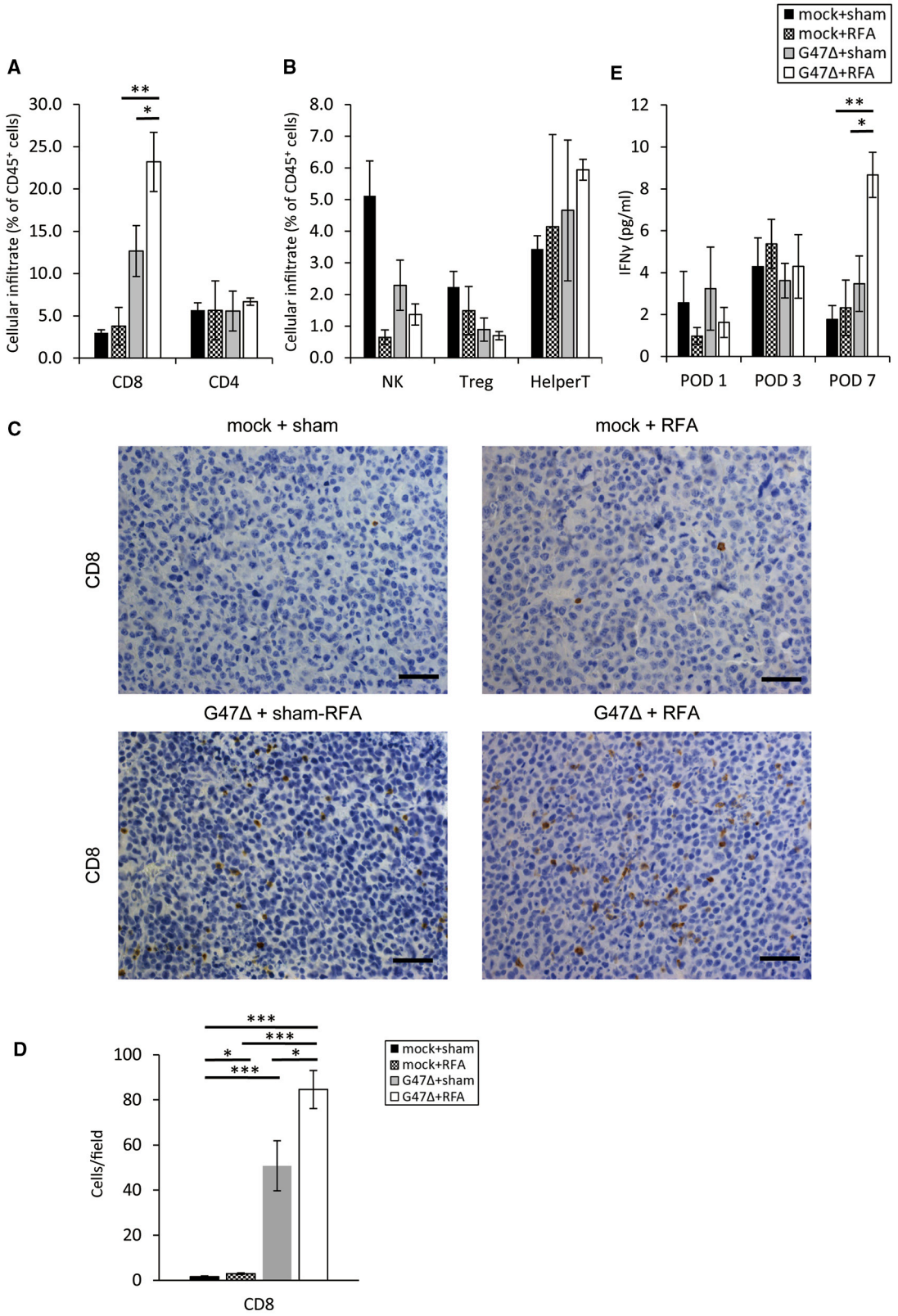

(legend on next page)

recurrence, established subcutaneous Neuro2a tumors on the left flank of A/J mice were injected with G47Δ (2×10^6 PFU) or mock on days 6, 8, and 10, followed by RFA on day 12. Mice were rechallenged with subcutaneous injection of Neuro2a cells (1×10^6) into the right flank on the same day of RFA administration, and tumor development was observed (Figure 5A). Tumors larger than 25 mm^3 were defined as engrafted. All mice in the RFA monotherapy group developed tumors after rechallenge, whereas three of the seven mice in the combination therapy group did not. The engraftment rate between the two groups was significantly different ($p = 0.03$; Figure 5B). To investigate whether the antitumor immunity conferred by neoadjuvant G47Δ remained after complete tumor ablation by RFA, IFN-γ secretion from splenocytes was evaluated by enzyme-linked immunospot (ELISPOT) assay on day 26. The mean number of Neuro2a tumor-reactive IFN-γ-secreting spots was significantly increased ($p < 0.05$) in the combination therapy group (95 spots/well) compared with the RFA monotherapy group (1.8 spots/well). There was no difference between the two groups when SaI/N cells were used as a control for stimulation (Figures 5C and 5D).

The Efficacy of the G47Δ + RFA Therapy Is Enhanced by an ICI Booster

Finally, we evaluated the effect of an anti-PD-1 ligand 1 (PD-L1) antibody used simultaneously with the G47Δ + RFA combination therapy. The anti-PD-L1 antibody (50 μg) was administered intraperitoneally on days 6, 9, 12, and 15 into A/J mice bearing bilateral subcutaneous Neuro2a tumors (Figure 6A). At the low dosage used, the anti-PD-L1 antibody alone showed no effect on tumor growth (Figure 6B). Also, the anti-PD-L1 antibody at this dosage did not show any enhancement of efficacy when combined with G47Δ or RFA (data not shown). However, anti-PD-L1 antibody treatment significantly enhanced the G47Δ + RFA combination therapy (Figure 6B). These results indicate that the neoadjuvant use of G47Δ enhances the efficacy of RFA via tumor-specific antitumor immunity that requires $CD8^+$ T cells, and such efficacy can be further augmented by the simultaneous use of ICIs.

DISCUSSION

RFA is a widely used treatment modality for a variety of tumors as well as non-neoplastic diseases. RFA is especially important for treating HCC, because, currently, it is the standard local treatment for HCC and has been reported to elicit an abscopal effect, that is, an antitumor effect on remote tumors presumably via antitumor immunity.[23,24] In the present study, however, RFA alone did not show any antitumor effect on the remote contralateral tumor in the bilateral subcutaneous Neuro2a tumor model. The reason is likely due to the poor immunogenicity of Neuro2a cells, whereas the abscopal effect of RFA has been observed in mouse models using immunogenic cell lines such as CT26 and BNL.[16,25] In patients with HCC, the abscopal effect of RFA is rarely observed and is considered irrelevant to patient prognosis.

Alternatively, oncolytic virus therapy using HSV-1 is known to induce systemic and specific antitumor immunity.[21] It has been shown in a phase III trial in patients with malignant melanoma that local injections with oncolytic HSV-1 can act on remote non-injected tumors via systemic antitumor immunity and even prolong the overall survival of patients.[6] G47Δ is specifically designed so that there is an enhanced stimulation of specific antitumor immune responses.[1] The biggest problem with the current RFA treatment for HCC is not the control of the treated lesions but its incapability to suppress the appearance of remote new lesions within the liver. Therefore, we hypothesized that neoadjuvant use of G47Δ would suppress the appearance of new lesions after RFA via efficient induction of specific antitumor immunity. In fact, we show that neoadjuvant G47Δ treatment in combination with RFA suppressed the tumor growth of contralateral tumors significantly better than did RFA alone. Furthermore, this augmented efficacy by neoadjuvant G47Δ is shown to require $CD8^+$ T cells by a depletion study using an anti-CD8 antibody. Evaluation of TILs in the contralateral tumors revealed that the percentage of $CD8^+$ T cells among $CD45^+$ cells was significantly increased when G47Δ was used as a neoadjuvant. Moreover, the neoadjuvant G47Δ treatment caused a significant increase in IFN-γ-secreting splenocytes, harvested 2 weeks after RFA, that reacted specifically to tumor cells. As immunological events that follow oncolytic virus treatments, several reports suggest the induction of immunogenic cell death and chemokines such as CXCL9 and CXCL10.[22,26–28] RFA induces heat shock proteins, which could work positively toward immune responses by G47Δ.[29] All of our data suggest that the mechanism of neoadjuvant G47Δ in augmenting the efficacy of RFA treatment is the induction of systemic and specific antitumor immunity. The results further indicate that G47Δ is likely useful as a neoadjuvant therapy for RFA in cancer patients, including HCC patients, in which the growth of non-treated lesions or the appearance of new lesions may be effectively suppressed.

In the present study, we initially sought to use tumor models of HCC, a cancer for which RFA is most commonly used, but all murine HCC

Figure 3. Flow Cytometric Analyses of TILs and Serum Cytokine Analyses in the G47Δ and RFA Combination Therapy

A/J mice with bilateral subcutaneous Neuro2a tumors were treated as scheduled in Figure 2A. (A) The right, non-treated tumors were collected on day 14, and immune cells infiltrating the subcutaneous tumors were evaluated by flow cytometry. The G47Δ + RFA therapy increased the proportion of $CD8^+$ T cells in the right tumors compared with each monotherapy. The data are means (n = 4-5); bars represent SEM. (B) The G47Δ + RFA therapy decreased the proportion of regulatory T cells in the right tumors compared with control but not with each monotherapy. (C) Immunohistological analysis of $CD8^+$ T cells in right tumors revealed a greater quantity of $CD8^+$ T cells infiltrating the tumor after the combination therapy. Scale bars, 50 μm. (D) $CD8^+$ cells were counted in five fields/section. (E) The G47Δ + RFA therapy increased serum IFN-γ levels. Serum was collected from the mice on days 13 (POD 1), 15 (POD 3), and 19 (POD 7). IFN-γ was measured using the Bio-Plex system. IFN-γ was significantly increased in the combination therapy compared with each monotherapy on POD 7 ($p < 0.05$). The data are means (n = 5); bars represent SEM. *$p < 0.05$, **$p < 0.01$, ***$p < 0.001$. POD, postoperative day.

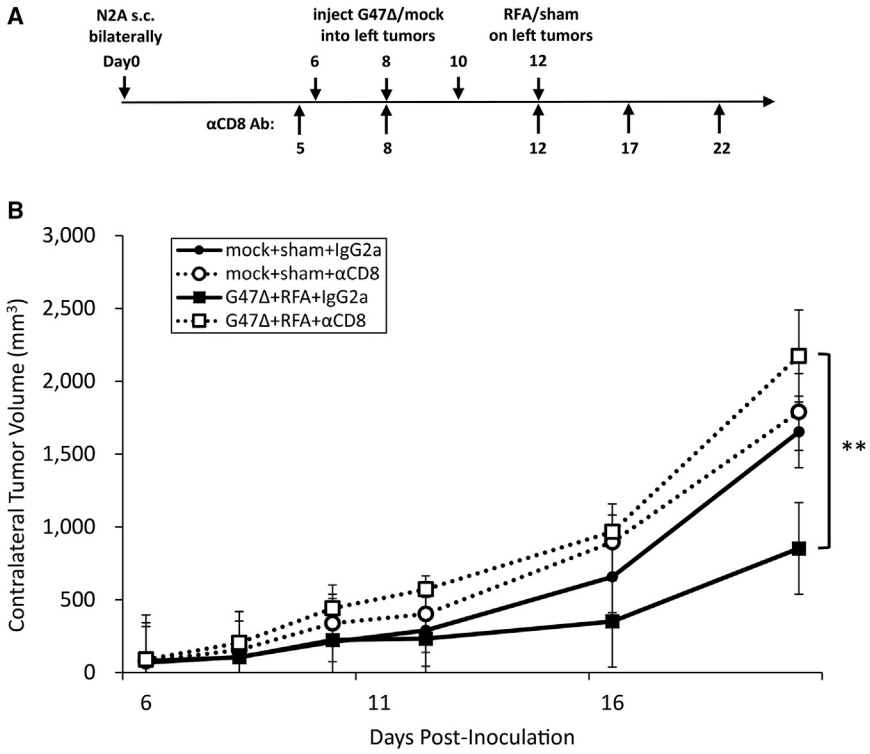

Figure 4. CD8⁺ T Cells Are Required for the Augmented Antitumor Efficacy of the G47Δ + RFA Combination Therapy

(A) In A/J mice with bilateral subcutaneous Neuro2a tumors, left tumors alone were treated with G47Δ + RFA and the contralateral tumor growth was followed. Anti-CD8 monoclonal or control rat IgG2a antibody was injected intraperitoneally five times as indicated. (B) The contralateral tumor volume was evaluated for tumor growth. The depletion of $CD8^+$ T cells completely abolished the augmented antitumor efficacy by the G47Δ and RFA combination therapy. The results are means (n = 7); bars represent SEM. $^{**}p < 0.01$.

cell lines available, including MH134-TC, the only murine HCC cell line that consistently formed subcutaneous tumors, were found to be too immunogenic in syngeneic mice for immunological studies. As a result of seeking a model, we show that G47Δ infects efficiently, exhibits cytopathic activities against, and replicates well in human HCC cells. Also, using athymic mice bearing HCC subcutaneously or orthotopically, we show that intratumoral injections with G47Δ cause a significant efficacy. G47Δ has been tested in multiple clinical trials and shown to be safe even when injected repeatedly into the human brain at a high dose of 10^9 PFU.[5] In clinical settings, most HCCs are easily accessed by ultrasonography-guided needle interventions, and therefore G47Δ should be useful for the treatment of human HCC.

Nivolumab for advanced HCC treatment showed durable objective responses in the CheckMate 040 study and is available for HCC treatment in many countries.[17] Several factors, such as the extent of cytotoxic T cell infiltration and the PD-L1 expression level on the surface of cancer cells, are reportedly useful for estimating the efficacy of ICIs.[30,31] Because the key feature of G47Δ is its high capability as an *in situ* vaccination where the cancer cells are efficiently recognized by the host immune system via cancer cell-specific virus replication, simultaneous administration of an ICI should augment the efficacy of G47Δ. In fact, we show that an anti-PD-L1 antibody, when used as a booster, significantly enhances the efficacy of the G47Δ and RFA combination therapy. The anti-PD-L1 antibody was used intentionally at a low dose of 50 μg, so that the antibody alone showed no effect on the growth of subcutaneous Neuro2a tumors.[32] Others have used an anti-CTLA-4 antibody or an anti-PD-1 antibody in combination with G47Δ armed with IL-12 and shown improvement of survival in a mouse glioma model.[21] Our results have an important clinical implication that the sequential use of G47Δ, RFA, and an ICI may be useful as a treatment strategy that can newly replace RFA monotherapy.

In conclusion, the neoadjuvant use of G47Δ can effectively enhance the efficacy of RFA via $CD8^+$ T cell-dependent antitumor immunity, which may be a practical therapeutic approach for patients treated with RFA, including those with liver cancer. The sequential use of G47Δ, RFA, and an ICI should further improve the antitumor efficacy.

MATERIALS AND METHODS

Cell Lines and Virus

Vero (African green monkey kidney), Hep3B (human HCC), SNU-398 (human HCC), and SaI/N (A/J mouse-derived fibrosarcoma) cell lines were purchased from the American Type Culture Collection. HuH-7 (human HCC), HepG2 (human HCC), and PLC/PRF/5 (human HCC) cell lines were purchased from the Japanese Collection of Research Bioresources. The Hepa1-6 (murine HCC) cell line was purchased from Riken Cell Bank. The MH134-TC (C3H mouse-derived HCC) cell line was purchased from the Cell Resource Center for Biomedical Research, Institute of Development, Aging and Cancer, Tohoku University. Neuro2a (A/J mouse-derived neuroblastoma) cells were purchased from the Health Science Research Resources Bank. Cells were maintained in DMEM or RPMI 1640 supplemented with 10% fetal bovine serum or 10% heat-inactivated fetal bovine serum at 37°C under 5% CO_2. G47Δ is a conditionally replicating oncolytic HSV-1 virus that was constructed as described previously.[1]

In Vitro Cytotoxicity Studies

In vitro cytotoxicity studies were performed as described previously.[33] The number of surviving cells was counted daily using a Coulter counter (Beckman Coulter, Pasadena, CA, USA) and expressed as the percentage of the number of mock-infected control cells.

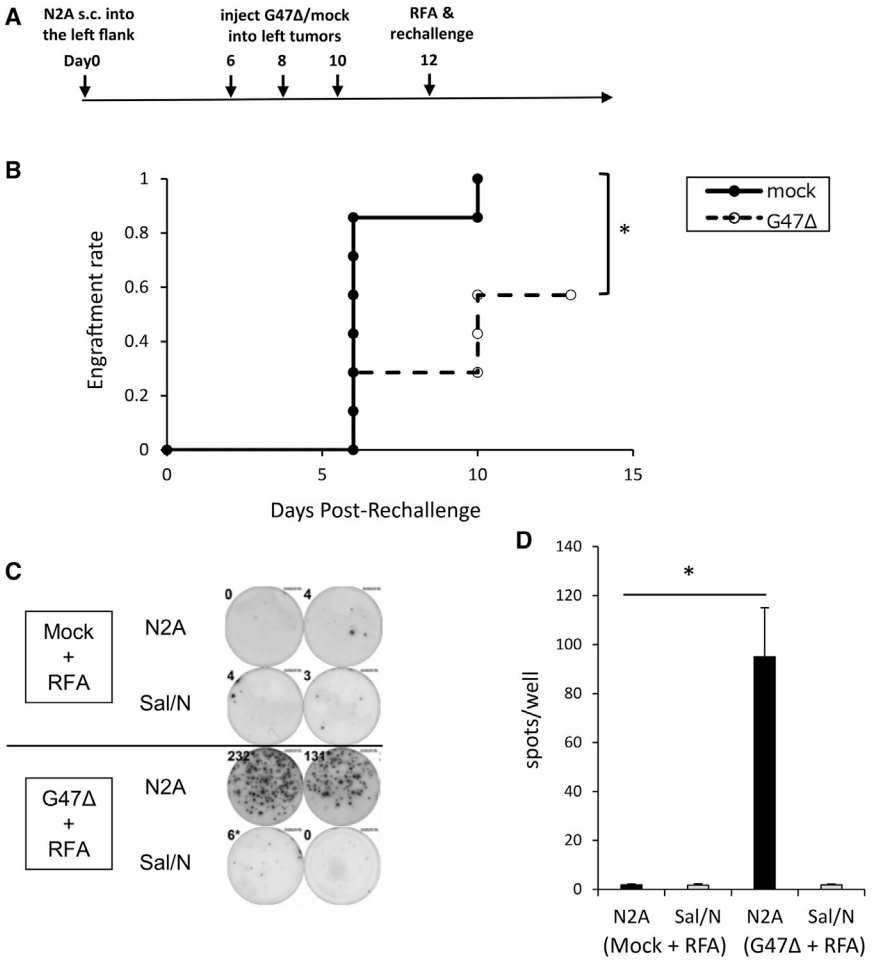

Figure 5. Neoadjuvant G47Δ in Combination with RFA Leads to Rejection of Tumor Rechallenge and Builds Tumor-Specific Antitumor Immunity

(A) Unilateral subcutaneous Neuro2a tumors were treated with RFA with or without neoadjuvant G47Δ treatment, and Neuro2a tumors were rechallenged on the contralateral flank. (B) Rechallenged tumors were evaluated for tumor growth. A tumor volume >25 mm^3 was defined as engrafted. The engraftment rate was significantly decreased by the combination therapy compared with RFA alone. (C) Without rechallenge, unilateral subcutaneous tumors were treated as in (A). Splenocytes were collected on day 26, stimulated with either Neuro2a cells or the control Sal/N cells, and subjected to ELISPOT assay of IFN-γ. Representative ELISPOT assay images are shown. (D) The mean number of IFN-γ-secreting spots stimulated by Neuro2a cells, but not by Sal/N cells, was significantly increased in the combination therapy group. The data are means (n = 5); bars represent SEM. *$p < 0.05$.

X-gal Staining

Vero cells, five human HCC cell lines (Hep3B, SNU-398, HuH-7, HepG2, and PLC/PRF/5), and a murine HCC cell line (Hepa1-6) were seeded in six-well plates (3×10^5/well) and infected with G47Δ at a MOI of 1 or 3 at 37°C for 1 h and incubated for another 4 h. Cells were fixed with 0.2% glutaraldehyde/2% paraformaldehyde and incubated with X-gal substrate solution (PBS, X-gal, 5 mM potassium ferricyanide, 5 mM potassium ferrocyanide, and 2 mM magnesium chloride) at 37°C for 2 h.

Virus Replication Assay

The five human HCC cell lines, Hepa1-6 cells, and Vero cells were seeded in six-well plates (3×10^5/well) and infected with G47Δ at a MOI of 0.01. After incubation at 37°C for 24 or 48 h, cells were collected and virus yields were assessed using Vero cells by a plaque assay.

Animal Studies

BALB/c *nu/nu* female mice (6–7 weeks old), A/J mice (5–7 weeks old), and C3H female mice (6 weeks old) were purchased from Japan SLC. All animal studies were approved by the Ethics Committee for Animal Experimentation of the University of Tokyo.

Subcutaneous Tumor Models

Subcutaneous tumors were generated by injecting HepG2 or Hep3B cells (5×10^6) into BALB/c *nu/nu* mice, MH134-TC cells (5×10^6) into syngeneic C3H mice, and Neuro2a cells (5×10^6) into syngeneic A/J mice; the cells were added to 70 μL of serum-free medium before subcutaneous injection into the left or bilateral flanks. When the subcutaneous tumors in the athymic mice reached 5 mm in diameter, G47Δ (2×10^6 PFU) or mock (defined as 20 μL of PBS supplemented with 10% glycerol) was administered intratumorally on days 0 and 3. Mice were sacrificed when tumors reached 20 mm in diameter in bilateral models and 24 mm in diameter in unilateral models as approved by the Ethics Committee for Animal Experimentation of the University of Tokyo.

Orthotopic Tumor Model

As an orthotopic mouse tumor model of liver cancer, several reports describe generating tumors in the liver by injecting HCC cells into the subcapsular space of the spleen.[34] Orthotopic HCC was generated in athymic mice by splenic subcapsular implantation of Hep3B cells (3×10^6) in 30 μL of serum-free medium as described previously, with modifications.[34] Tumors were treated with an intratumoral injection of G47Δ or the mock treatment on day 35.

Neoadjuvant G47Δ Therapy and ICI Booster

A/J mice with bilateral Neuro2a tumors were treated with intratumoral injections with G47Δ (2×10^6 PFU) in the left-side tumors on days 6, 8, and 10, followed by RFA on day 12. For the ICI experiment, 50 μg of anti-PD-L1 antibody (clone 10F.9G2, Bio X Cell, West Lebanon, NH, USA) or isotype control antibody (rat IgG2b clone LTF-2, Bio X Cell, West Lebanon, NH, USA) was administered

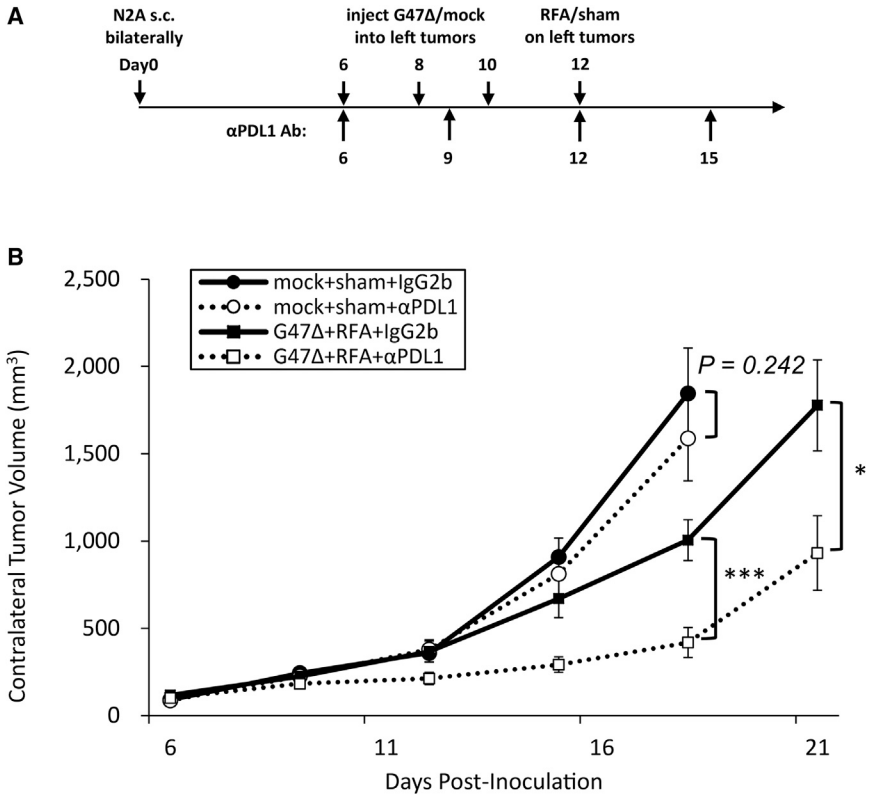

Figure 6. An Anti-PD-L1 Antibody Enhances the Efficacy of the G47Δ + RFA Combination

(A) Bilateral subcutaneous Neuro2a tumors were established in A/J mice, and the left tumors were treated with G47Δ (2×10^6 PFU) and RFA, and the tumor growth on the right side was followed. An anti-PD-L1 or control rat IgG2b antibody was injected intraperitoneally four times as indicated. (B) The contralateral tumor volume was evaluated for tumor growth. Addition of an anti-PD-L1 antibody significantly enhanced the efficacy of the G47Δ + RFA therapy. The data are means (n = 7); bars represent SEM. *$p < 0.05$, ***$p < 0.001$.

intraperitoneally on days 6, 9, 12, and 15. For $CD8^+$ T cell depletion, 250 μg of anti-CD8 antibody (clone 53-6.82, BioXCell, West Lebanon, NH, USA) or the isotype control antibody (rat IgG2a clone 2A3, Bio X Cell, West Lebanon, NH, USA) was administered intraperitoneally on days 5, 8, 12, 17, and 22. Tumor growth was determined by measuring the tumor volume (length × width × height × $^1/_2$) twice weekly. Animals were sacrificed when the maximum diameter of the tumor on either side reached 20 mm.

Combination drug interactions were determined based on a previously reported method.[35] The FTV was calculated as the experimental tumor volume/mean control tumor volume. The expected FTV was calculated as the FTV after RFA × FTV after G47Δ. If the ratio of the expected FTV to observed FTV is greater than 1, the effect is expected to be synergistic. A ratio less than 1 suggests that the effect is additive.

RFA Application

Subcutaneous tumors were treated with RFA using the VIVA RF generator and electrode (STARmed, Goyang, Republic of Korea). An active electrode (5 mm long) was inserted directly into the tumor for ablation at 5 W for 60–80 s.

Flow Cytometric Analysis

For extraction of TILs, mice bearing bilateral subcutaneous Neuro2a tumors were treated with G47Δ (2×10^6 PFU) on days 6, 8, and 10, followed by RFA on day 12, and contralateral tumors were removed on day 14. A mouse tumor dissociation kit, gentleMACS dissociator, and gentleMACS C tubes (Miltenyi Biotec, Bergisch Gladbach, Germany) were used to prepare single tumor cells according to the manufacturer's protocol. Red blood cells (RBCs) were removed using RBC lysis buffer (eBioscience, Santa Clara, CA, USA). TILs were stained with several antibodies (see Table S1) and analyzed following the gating strategy (see Figure S2A). For intranuclear staining, the True-Nuclear transcription factor buffer set (BioLegend, San Diego, CA, USA) was used according to the manufacturer's protocol. Flow cytometric analysis was performed on the CytoFLEX flow cytometer (Beckman Coulter, Pasadena, CA, USA).

Histological Analyses

Mice were sacrificed on day 14, and tumors were fixed in 10% formaldehyde neutral buffer solution (Sigma-Aldrich, St. Louis, MO, USA) for 72 h and embedded in paraffin. Sections were rehydrated through an alcohol gradient and subjected to heat-mediated antigen retrieval using target retrieval solution S1700 (Dako, Santa Clara, CA, USA). The sections were stained with an anti-mouse CD8 antibody (Abcam, Cambridge, UK) followed by 3,3′-diaminobenzidine as the chromogenic substrate. For semiquantitative analysis, positive cells were counted in five fields/section.

Cytokine analysis

Serum collected from mice on days 13, 15, and 19 was used for cytokine analysis. The levels of IFN-γ, IL-12, and IL-6 were evaluated using the Bio-Plex multiplex assay and Bio-Plex 200 system (Bio-Rad, Hercules, CA, USA) according to the manufacturer's protocol.

Rechallenge Studies

Neuro2a cells (5×10^6) were implanted subcutaneously into the left flanks of A/J mice, and the resulting tumors were injected intratumorally with G47Δ (2×10^6 PFU) or mock treatment on days 6, 8, and 10, followed by RFA on day 12. Whereas 5×10^6 cells, larger than the minimal number, are used for rapid establishment of

subcutaneous Neuro2a tumors, the minimum number of cells that gives 100% engraftment is found to be 1×10^6 according to our preliminary experiments (data not shown). Therefore, mice were re-challenged with subcutaneous implantation of 1×10^6 Neuro2a cells into the contralateral right flanks on the same day of RFA administration, and tumor growth was observed twice a week. Because we observe that subcutaneous Neuro2a tumors do not regress spontaneously once they exceed 25 mm^3, tumors larger than 25 mm^3 were defined as engrafted, and the rate of tumor engraftment was determined.

ELISPOT Assay

Neuro2a cells (5×10^6) were implanted subcutaneously into the left flanks of A/J mice, and the resulting tumors were injected intratumorally with G47Δ (2×10^6 PFU) or mock on days 6, 8, and 10, followed by RFA on day 12. Mice were sacrificed on day 26, and a single-cell suspension of splenocytes was prepared. After the splenocytes were stimulated by Neuro2a or SaI/N cells, IFN-γ secretion from tumor-reactive splenocytes was evaluated using an IFN-γ ELISpot^{PLUS} kit (Mabtech, Nacka Strand, Sweden). Assays were conducted following the manufacturer's protocol. Specific spots were counted and analyzed using the ImmunoSpot analyzer and ImmunoSpot software (CTL, Cleveland, OH, USA).

Statistical Analysis

Two-tailed Student's t tests were used for all comparisons, except those of overall survival and engraftment rate, for which the log-rank test was used. In all cases, $p < 0.05$ was considered to indicate significance. All statistical analyses were performed using JMP Pro 14.

SUPPLEMENTAL INFORMATION

Supplemental Information can be found online at https://doi.org/10.1016/j.omto.2020.08.010.

AUTHOR CONTRIBUTIONS

T.Y. and T.T. were involved with the conception, design, and performance of experiments, statistical analyses, interpretation of results, and writing the manuscript. M.I. assisted with designing and performing the experiments. R.T. and K.K. were involved with the conception and design of experiments. All authors reviewed and edited the manuscript.

CONFLICTS OF INTEREST

T.T. owns the patent right for G47Δ in Japan. The remaining authors declare no competing interests.

ACKNOWLEDGMENTS

We thank Dr. Yasushi Ino for his advice in planning experiments. This research is supported in part by grants to T.T. from Practical Research for Innovative Cancer Control, Japan Agency for Medical Research and Development (AMED) (grant no. JP19ck0106416) and the Translational Research Program, AMED (grant no. JP19lm0203004).

REFERENCES

1. Todo, T., Martuza, R.L., Rabkin, S.D., and Johnson, P.A. (2001). Oncolytic herpes simplex virus vector with enhanced MHC class I presentation and tumor cell killing. Proc. Natl. Acad. Sci. USA *98*, 6396–6401.
2. Fukuhara, H., Martuza, R.L., Rabkin, S.D., Ito, Y., and Todo, T. (2005). Oncolytic herpes simplex virus vector g47Δ in combination with androgen ablation for the treatment of human prostate adenocarcinoma. Clin. Cancer Res. *11*, 7886–7890.
3. Cheema, T.A., Wakimoto, H., Fecci, P.E., Ning, J., Kuroda, T., Jeyaretna, D.S., Martuza, R.L., and Rabkin, S.D. (2013). Multifaceted oncolytic virus therapy for glioblastoma in an immunocompetent cancer stem cell model. Proc. Natl. Acad. Sci. USA *110*, 12006–12011.
4. Wang, J.N., Xu, L.H., Zeng, W.G., Hu, P., Rabkin, S.D., and Liu, R.R. (2015). Treatment of human thyroid carcinoma cells with the g47delta oncolytic herpes simplex virus. Asian Pac. J. Cancer Prev. *16*, 1241–1245.
5. Fukuhara, H., Ino, Y., and Todo, T. (2016). Oncolytic virus therapy: a new era of cancer treatment at dawn. Cancer Sci. *107*, 1373–1379.
6. Andtbacka, R.H.I., Kaufman, H.L., Collichio, F., Amatruda, T., Senzer, N., Chesney, J., Delman, K.A., Spitler, L.E., Puzanov, I., Agarwala, S.S., et al. (2015). Talimogene laherparepvec improves durable response rate in patients with advanced melanoma. J. Clin. Oncol. *33*, 2780–2788.
7. Desjardins, A., Gromeier, M., Herndon, J.E., 2nd, Beaubier, N., Bolognesi, D.P., Friedman, A.H., Friedman, H.S., McSherry, F., Muscat, A.M., Nair, S., et al. (2018). Recurrent glioblastoma treated with recombinant poliovirus. N. Engl. J. Med. *379*, 150–161.
8. Heo, J., Reid, T., Ruo, L., Breitbach, C.J., Rose, S., Bloomston, M., Cho, M., Lim, H.Y., Chung, H.C., Kim, C.W., et al. (2013). Randomized dose-finding clinical trial of oncolytic immunotherapeutic vaccinia JX-594 in liver cancer. Nat. Med. *19*, 329–336.
9. Song, T.J., Eisenberg, D.P., Adusumilli, P.S., Hezel, M., and Fong, Y. (2006). Oncolytic herpes viral therapy is effective in the treatment of hepatocellular carcinoma cell lines. J. Gastrointest. Surg. *10*, 532–542.
10. Nakatake, R., Kaibori, M., Nakamura, Y., Tanaka, Y., Matushima, H., Okumura, T., Murakami, T., Ino, Y., Todo, T., and Kon, M. (2018). Third-generation oncolytic herpes simplex virus inhibits the growth of liver tumors in mice. Cancer Sci. *109*, 600–610.
11. Tatli, S., Tapan, U., Morrison, P.R., and Silverman, S.G. (2012). Radiofrequency ablation: technique and clinical applications. Diagn. Interv. Radiol. *18*, 508–516.
12. Tateishi, R., Shiina, S., Ohki, T., Sato, T., Masuzaki, R., Imamura, J., Goto, E., Goto, T., Yoshida, H., Obi, S., et al. (2009). Treatment strategy for hepatocellular carcinoma: expanding the indications for radiofrequency ablation. J. Gastroenterol. *44* (*Suppl 19*), 142–146.
13. Shiina, S., Tateishi, R., Arano, T., Uchino, K., Enooku, K., Nakagawa, H., Asaoka, Y., Sato, T., Masuzaki, R., Kondo, Y., et al. (2012). Radiofrequency ablation for hepatocellular carcinoma: 10-year outcome and prognostic factors. Am. J. Gastroenterol. *107*, 569–577, quiz 578.
14. Ahmed, M., Kumar, G., Moussa, M., Wang, Y., Rozenblum, N., Galun, E., and Goldberg, S.N. (2016). Hepatic radiofrequency ablation-induced stimulation of distant tumor growth is suppressed by c-Met inhibition. Radiology *279*, 103–117.
15. Behm, B., Di Fazio, P., Michl, P., Neureiter, D., Kemmerling, R., Hahn, E.G., Strobel, D., Gress, T., Schuppan, D., and Wissniowski, T.T. (2016). Additive antitumour response to the rabbit VX2 hepatoma by combined radio frequency ablation and toll like receptor 9 stimulation. Gut *65*, 134–143.
16. Shi, L., Chen, L., Wu, C., Zhu, Y., Xu, B., Zheng, X., Sun, M., Wen, W., Dai, X., Yang, M., et al. (2016). PD-1 blockade boosts radiofrequency ablation-elicited adaptive immune responses against tumor. Clin. Cancer Res. *22*, 1173–1184.
17. El-Khoueiry, A.B., Sangro, B., Yau, T., Crocenzi, T.S., Kudo, M., Hsu, C., Kim, T.Y., Choo, S.P., Trojan, J., Welling, T.H., et al. (2017). Nivolumab in patients with advanced hepatocellular carcinoma (CheckMate 040): an open-label, non-comparative, phase 1/2 dose escalation and expansion trial. Lancet *389*, 2492–2502.
18. Mizukoshi, E., Yamashita, T., Arai, K., Sunagozaka, H., Ueda, T., Arihara, F., Kagaya, T., Yamashita, T., Fushimi, K., and Kaneko, S. (2013). Enhancement of tumor-associated antigen-specific T cell responses by radiofrequency ablation of hepatocellular carcinoma. Hepatology *57*, 1448–1457.

19. den Brok, M.H.M.G.M., Sutmuller, R.P.M., van der Voort, R., Bennink, E.J., Figdor, C.G., Ruers, T.J., and Adema, G.J. (2004). In situ tumor ablation creates an antigen source for the generation of antitumor immunity. Cancer Res. *64*, 4024–4029.

20. Ribas, A., Dummer, R., Puzanov, I., VanderWalde, A., Andtbacka, R.H.I., Michielin, O., Olszanski, A.J., Malvehy, J., Cebon, J., Fernandez, E., et al. (2017). Oncolytic virotherapy promotes intratumoral T cell infiltration and improves anti-PD-1 immunotherapy. Cell *170*, 1109–1119.e10.

21. Saha, D., Martuza, R.L., and Rabkin, S.D. (2017). Macrophage polarization contributes to glioblastoma eradication by combination immunovirotherapy and immune checkpoint blockade. Cancer Cell *32*, 253–267.e5.

22. Bourgeois-Daigneault, M.-C., Roy, D.G., Aitken, A.S., El Sayes, N., Martin, N.T., Varette, O., Falls, T., St-Germain, L.E., Pelin, A., Lichty, B.D., et al. (2018). Neoadjuvant oncolytic virotherapy before surgery sensitizes triple-negative breast cancer to immune checkpoint therapy. Sci. Transl. Med. *10*, 1–12.

23. Wissniowski, T.T., Hänsler, J., Neureiter, D., Frieser, M., Schaber, S., Esslinger, B., Voll, R., Strobel, D., Hahn, E.G., and Schuppan, D. (2003). Activation of tumor-specific T lymphocytes by radio-frequency ablation of the VX2 hepatoma in rabbits. Cancer Res. *63*, 6496–6500.

24. Dromi, S.A., Walsh, M.P., Herby, S., Traughber, B., Xie, J., Sharma, K.V., Sekhar, K.P., Luk, A., Liewehr, D.J., Dreher, M.R., et al. (2009). Radiofrequency ablation induces antigen-presenting cell infiltration and amplification of weak tumor-induced immunity. Radiology *251*, 58–66.

25. Iida, N., Nakamoto, Y., Baba, T., Nakagawa, H., Mizukoshi, E., Naito, M., Mukaida, N., and Kaneko, S. (2010). Antitumor effect after radiofrequency ablation of murine hepatoma is augmented by an active variant of CC chemokine ligand 3/macrophage inflammatory protein-1α. Cancer Res. *70*, 6556–6565.

26. van Vloten, J.P., Workenhe, S.T., Wootton, S.K., Mossman, K.L., and Bridle, B.W. (2018). Critical interactions between immunogenic cancer cell death, oncolytic viruses, and the immune system define the rational design of combination immunotherapies. J. Immunol. *200*, 450–458.

27. Spranger, S., Dai, D., Horton, B., and Gajewski, T.F. (2017). Tumor-residing Batf3 dendritic cells are required for effector T cell trafficking and adoptive T cell therapy. Cancer Cell *31*, 711–723.e4.

28. Melcher, A., Parato, K., Rooney, C.M., and Bell, J.C. (2011). Thunder and lightning: immunotherapy and oncolytic viruses collide. Mol. Ther. *19*, 1008–1016.

29. Yoo, J.Y., Hurwitz, B.S., Bolyard, C., Yu, J.G., Zhang, J., Selvendiran, K., Rath, K.S., He, S., Bailey, Z., Eaves, D., et al. (2014). Bortezomib-induced unfolded protein response increases oncolytic HSV-1 replication resulting in synergistic antitumor effects. Clin. Cancer Res. *20*, 3787–3798.

30. Teng, M.W.L., Ngiow, S.F., Ribas, A., and Smyth, M.J. (2015). Classifying cancers based on T-cell infiltration and PD-L1. Cancer Res. *75*, 2139–2145.

31. Tumeh, P.C., Harview, C.L., Yearley, J.H., Shintaku, I.P., Taylor, E.J.M., Robert, L., Chmielowski, B., Spasic, M., Henry, G., Ciobanu, V., et al. (2014). PD-1 blockade induces responses by inhibiting adaptive immune resistance. Nature *515*, 568–571.

32. Srinivasan, P., Wu, X., Basu, M., Rossi, C., and Sandler, A.D. (2018). PD-L1 checkpoint inhibition and anti-CTLA-4 whole tumor cell vaccination counter adaptive immune resistance: a mouse neuroblastoma model that mimics human disease. PLoS Med. *15*, e1002497.

33. Todo, T., Rabkin, S.D., Sundaresan, P., Wu, A., Meehan, K.R., Herscowitz, H.B., and Martuza, R.L. (1999). Systemic antitumor immunity in experimental brain tumor therapy using a multimutated, replication-competent herpes simplex virus. Hum. Gene Ther. *10*, 2741–2755.

34. Kim, J., Won, R., Ban, G., Ju, M.H., Cho, K.S., Young Han, S., Jeong, J.S., and Lee, S.W. (2015). Targeted regression of hepatocellular carcinoma by cancer-specific RNA replacement through microRNA regulation. Sci. Rep. *5*, 12315.

35. Yu, D.C., Chen, Y., Dilley, J., Li, Y., Embry, M., Zhang, H., Nguyen, N., Amin, P., Oh, J., and Henderson, D.R. (2001). Antitumor synergy of CV787, a prostate cancer-specific adenovirus, and paclitaxel and docetaxel. Cancer Res. *61*, 517–525.

OMTO, Volume *18*

Supplemental Information

Neoadjuvant Use of Oncolytic Herpes Virus G47Δ Enhances the Antitumor Efficacy of Radiofrequency Ablation

Tomoharu Yamada, Ryosuke Tateishi, Miwako Iwai, Kazuhiko Koike, and Tomoki Todo

(A)

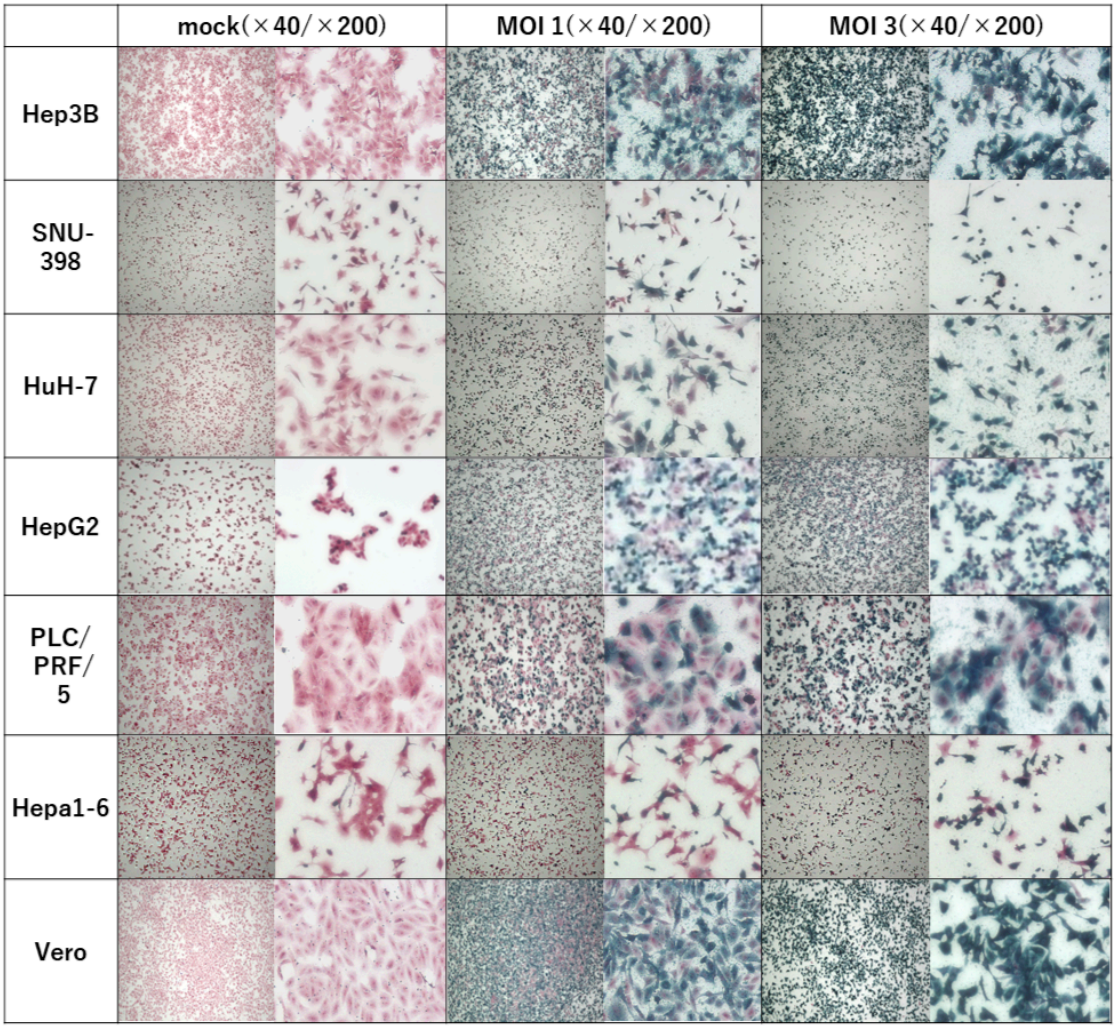
mock(×40/×200)
MOI 1(×40/×200)
MOI 3(×40/×200)
Hep3B
SNU-398
HuH-7
HepG2
PLC/PRF/5
Hepa1-6
Vero

(B)

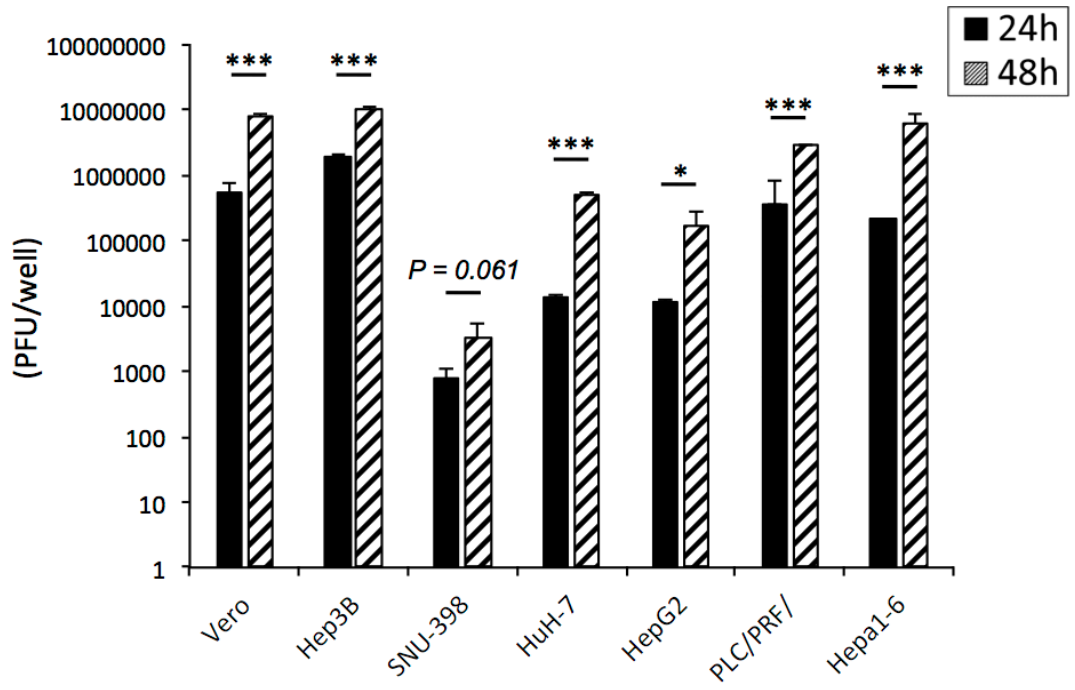
24h
48h
(PFU/well)
100000000
10000000
1000000
100000
10000
1000
100
10
1
***
***
P = 0.061
***
*
***
***
Vero
Hep3B
SNU-398
HuH-7
HepG2
PLC/PRF/
Hepa1-6

Supplementary Fig. S1

In vitro X-gal staining and virus replication assay

(A) Hep3B, SNU-398, HuH-7, HepG2, PLC/PRF/5, Hepa1-6 and Vero cell monolayers were infected with G47Δ at a MOI of 1 or 3, incubated for 6 hours, fixed, and stained with X-gal. (B) The cell monolayers were infected with G47Δ (3×10^3 pfu) and incubated at 37°C for 24 or 48 hours. Virus yields were evaluated by plaque assay on Vero cells. The data are means (n = 3); bars represent SD. *, $P < 0.05$. ***, $P < 0.001$.

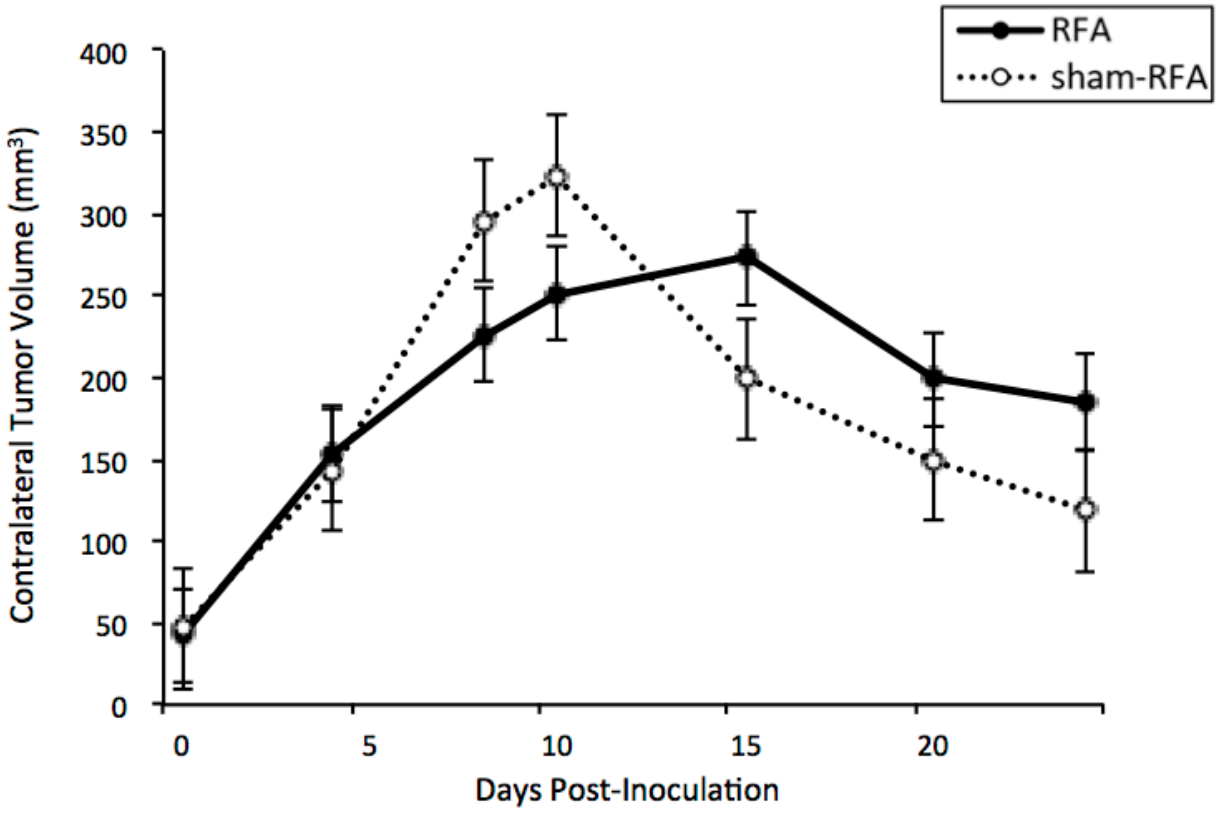

Supplementary Fig. S2

MH134-TC is too immunogenic to evaluate the antitumor efficacy of G47Δ in combination with RFA

MH134-TC was inoculated subcutaneously on bilateral flanks, and when tumors reached 6–8mm in diameter, the left tumors were treated with RFA or sham-RFA on day 4. Contralateral tumor volume was evaluated. Regardless of whether RFA was performed, all contralateral tumors eventually shrank. The data are means (n = 7); bars represent SEM.

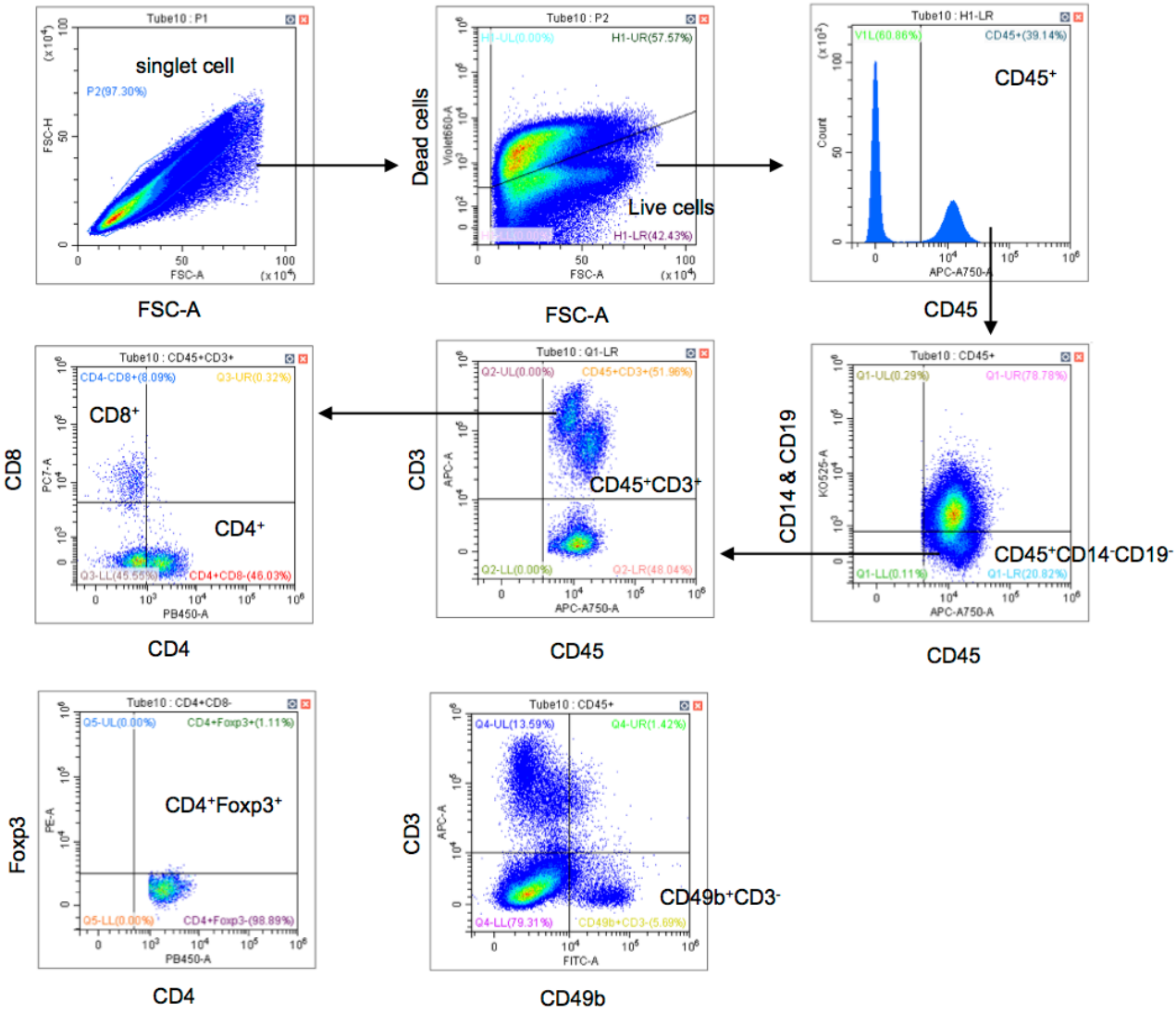

Supplementary Fig. S3

Determination of tumor-infiltrating lymphocytes (TILs) subsets by a flow cytometry gating strategy

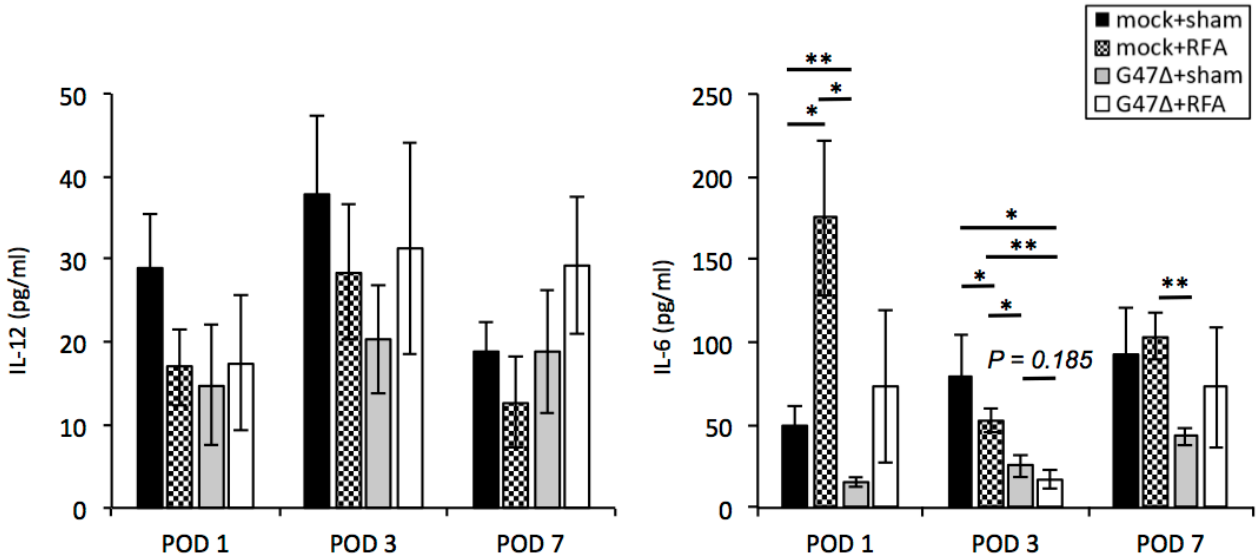

Supplementary Fig. S4

Serum cytokine analyses of the G47Δ and RFA combination therapy

The left subcutaneous Neuro2a tumors (average 78 mm^3) were treated as described in Fig. 2A. The serum was collected on days 13 (POD 1), 15 (POD 3) and 19 (POD 7). Levels of interleukin (IL)-12 and IL-6 were measured using the BioPlex system. For IL-12, the combination therapy did not cause any significant difference between other therapies. The combination therapy significantly decreased the IL-6 level compared with RFA monotherapy on POD 3. The data are means (n = 5); bars represent SEM. *, $P < 0.05$. **, $P < 0.01$.

Description	Fluorochromes	company
anti-mouse CD49b	FITC	BioLegend
anti-mouse Foxp3	PE	eBioscience
anti-mouse CD8a	PE/cy7	BioLegend
anti-mouse CD3	APC	BioLegend
anti-mouse CD45	APC/cy7	BioLegend
anti-mouse CD4	BV421	BioLegend
anti-mouse CD14	BV510	BioLegend
anti-mouse CD19	BV510	BioLegend
Fixable Viability Dye	BV570	BioLegend
Purified Anti-mouse CD16/32		BioLegend

Supplementary Table S1

The antibodies used in the flow cytometric analysis